HHS Public Access

Author manuscript

J Vasc Interv Radiol. Author manuscript; available in PMC 2015 May 01.

Published in final edited form as:

J Vasc Interv Radiol. 2015 May ; 26(5): 670–678.e2. doi:10.1016/j.jvir.2014.11.020.

Three-Dimensional Quantitative Assessment of Uterine Fibroid Response after Uterine Artery Embolization Using Contrast-Enhanced MR Imaging

Julius Chapiro, MD, **Rafael Duran, MD**, **MingDe Lin, PhD**, **John D. Werner, MD**, **Zhijun Wang, MD, PhD**, **Rüdiger Schernthaner, MD**, **Lynn Jeanette Savic, BS**, **Mark L. Lessne, MD**, **Jean-François Geschwind, MD**, and **Kelvin Hong, MD**

Russell H. Morgan Department of Radiology and Radiological Science, Division of Vascular and Interventional Radiology (J.C., R.D., J.D.W., R.S., L.J.S., M.L.L., J.-F.G., K.H., Z.W.), The Johns Hopkins Hospital, Sheikh Zayed Tower, Suite 7203, 1800 Orleans Street, Baltimore, MD 21287; Department of Diagnostic and Interventional Radiology (J.C., L.J.S.), Charité Universitätsmedizin, Berlin, Germany; and Clinical Informatics, Interventional, and Translational Solutions (M.L.), Philips Research North America, Briarcliff Manor, New York

Abstract

Purpose—To evaluate the clinical feasibility and diagnostic accuracy of three-dimensional (3D) quantitative magnetic resonance (MR) imaging for the assessment of total lesion volume (TLV) and enhancing lesion volume (ELV) before and after uterine artery embolization (UAE).

Materials and Methods—This retrospective study included 25 patients with uterine fibroids who underwent UAE and received contrast-enhanced MR imaging before and after the procedure. TLV was calculated using a semiautomated 3D segmentation of the dominant lesion on contrast-enhanced MR imaging, and ELV was defined as voxels within TLV where the enhancement exceeded the value of a region of interest placed in hypoenhancing soft tissue (left psoas muscle). ELV was expressed in relative (% of TLV) and absolute (in cm^3) metrics. Results were compared with manual measurements and correlated with symptomatic outcome using a linear regression model.

Results—Although 3D quantitative measurements of TLV demonstrated a strong correlation with the manual technique (R^2 = 0.93), measurements of ELV after UAE showed significant disagreement between techniques (R^2 = 0.72; residual standard error, 15.8). Six patients (24%) remained symptomatic and were classified as nonresponders. When stratified according to response, no difference in % ELV between responders and nonresponders was observed. When

Address correspondence to K.H.; khong1@jhmi.edu.

From the SIR 2014 Annual Meeting.

M.L. is an employee of Philips Research North America. M.L.L. is a paid consultant for AprioMed and has received a research grant from Merit Medical. J.-F.G. is a paid consultant for BTG, Bazer, Guerbet, Nordion, Philips Research North America, and Jennerex and has received research grants from the National Institutes of Health, Department of Defense, Philips Research North America, Threshold, Bayer HealthCare, and BTG. None of the other authors have identified a conflict of interest.

Appendix A and Figure E1 are available online at www.jvir.org.

assessed using cm^3 ELV, responders showed a significantly lower mean ELV compared with nonresponders (4.1 cm^3 [range, 0.3–19.8 cm^3] vs 77 cm^3 [range, 11.91–296 cm^3]; $P < .01$).

Conclusions—The use of segmentation-based 3D quantification of lesion enhancement is feasible and diagnostically accurate and could be considered as an MR imaging response marker for clinical outcome after UAE.

Over the past 15 years, the role of uterine artery embolization (UAE) has evolved as a well-accepted, safe, and effective alternative to surgical treatment in the management of uterine fibroids (1–5). UAE causes irreversible ischemic injury to fibroids, while maintaining endometrial perfusion, which is known to return to normal within 4 months after treatment (6,7). Ideally, this selective infarction leads to complete fibroid necrosis and, over time, to a reduction of fibroid volume (8). The extent of necrosis has been shown to correlate with symptomatic relief (9), and multiple studies have demonstrated that incomplete infarction may be the cause for poor clinical response, requiring repeat embolization (10–13).

Although clinical improvement remains the ultimate goal of treatment and represents the most powerful endpoint in most clinical trials, magnetic resonance (MR) imaging may be an important surrogate and predictive marker for treatment success (9,14). The radiologic evaluation of treatment response to UAE usually relies on individual anatomic measurements of fibroid volume by using the formula for a prolate ellipse (13). In addition, visual assessment of contrast enhancement on T1-weighted follow-up images serves as a measure of fibroid perfusion and viability (9,13). These methods rely on the assumption that fibroid growth or response to UAE occurs in a symmetric, spherical manner and can be reliably measured by subjective, visual assessment. However, little is known about the reliability and reproducibility of these methods, and more recent data questioned the predictive value of these subjective assessment techniques (15).

The present study evaluated the clinical feasibility and diagnostic accuracy of a semiautomated, three-dimensional (3D) quantitative MR imaging technique to assess uterine fibroid response after UAE by measuring total lesion volume (TLV) and enhancing lesion volume (ELV) on contrast-enhanced MR imaging.

MATERIALS AND METHODS

Study Cohort and Clinical Evaluation

This retrospective single-institution study was conducted in compliance with the Health Insurance Portability and Accountability Act, approved by the institutional review board, and designed in agreement with the Standards for Reporting of Diagnostic Accuracy (16). A retrospective review was performed of 91 consecutive patients with symptomatic uterine fibroids who underwent their first UAE procedure between December 2010 and December 2012. Patients without follow-up MR imaging (n = 52), patients who were treated with myomectomy after UAE (n = 11), and patients with significant motion artifacts on MR imaging (n = 3) were excluded from the final cohort, which consisted of 25 patients.

All included patients underwent baseline assessment by a referring gynecologist and an interventional radiologist. The patients were assessed regarding clinical symptoms based on

the Uterine Fibroid Symptom and Quality-of-Life Questionnaire (17). Patients presenting with menorrhagia or bulk-related symptoms (including pelvic pressure and pain, leg and back pain, heaviness or discomfort, urinary frequency or incontinence, abdominal bloating, constipation, and dyspareunia) were included in the analysis. After the procedure, all included patients presented for a clinical follow-up evaluation at 1 month and then at 6–8 months after treatment. The severity of symptoms was characterized as worsened, unchanged, improved, or resolved. Based on the clinical severity of symptoms recorded during the second follow-up visit, patients were classified as responders or nonresponders.

Embolization Procedure

An interventional radiologist with 10 years of experience in interventional radiology (K.H.) performed all embolization procedures. Briefly, a unilateral femoral access was achieved, and multiple angiographic steps were performed to define the uterine arterial anatomy. Consecutive direct selective catheterization of both uterine arteries was performed in all cases during the same procedure. First, the main uterine artery was engaged on one side using a Roberts uterine catheter (Cook, Inc, Bloomington, Indiana). Embolization of the uterine fibroids was performed through a coaxially advanced microcatheter (Renegade HI-FLO microcatheter; Boston Scientific, Marlborough, Massachusetts) using 500–900 μm microspheres (Embosphere; Merit Medical Systems, Inc, South Jordan, Utah). The angiographic endpoint was devascularization of the fibroid (complete lack of angiographic contrast material uptake) while preserving antegrade flow in the main uterine artery. The same technique was used to treat the contralateral side.

MR Imaging Technique

All patients included in the study underwent a standardized MR imaging protocol before and after UAE. Baseline MR imaging was acquired within 3 months before intraarterial therapy, and follow-up MR imaging was performed within a median of 6 months (range, 5–8 mo) after the procedure. MR imaging was performed on a 1.5-tesla scanner (CV/i; General Electric Medical Systems, Milwaukee, Wisconsin) using a phased array surface coil. The imaging protocol consisted of T2-weighted fast spin echo images (matrix, 256 × 256; slice thickness, 8 mm; intersection gap, 2 mm; repetition time/echo time, 5,000 ms/100 ms; receiver bandwidth, 32 kHz) and breath-hold unenhanced and contrast-enhanced (0.1 mmol/kg intravenous gadodiamide [Omniscan; GE Healthcare Bio-Sciences Corp, Piscataway, New Jersey]) T1-weighted 3D fat-suppressed spoiled gradient echo images (matrix, 192 × 160; slice thickness, 4–6 mm; receiver bandwidth, 64 kHz; flip angle, 15 degrees) that covered the whole uterus and were used to determine the viability of the uterine fibroids and the surrounding uterine tissue.

Imaging Data Evaluation

Subjective image analysis was performed by two radiologists with 6 and 7 years of experience in abdominal MR imaging (R.D., J.D.W.) who were not involved in the UAE procedure. Both readers were blinded to the results from the semiautomated, 3D quantitative image analysis, which was performed by a radiology resident (J.C.) who had 1 year of experience with the software prototype (described subsequently and in Appendix A, available online at www.jvir.org). All radiologic readers individually evaluated the entire

dataset. The values recorded by both non-3D readers were averaged and used for analysis and comparison with the 3D analysis. Any remaining ambiguity was resolved by consensus. T2-weighted baseline images were used to determine the number and location of the uterine fibroids. In each patient, the largest fibroid by volume was defined as the dominant lesion. Volumetric measurements of the dominant lesions on baseline and follow-up MR imaging were implemented using the formula for an ellipsoid (length × width × height × 0.523). Fibroid enhancement as a surrogate marker for lesion viability was visually assessed using baseline and follow-up contrast-enhanced MR imaging. The percentage of enhancement was recorded subjectively in 5% increments, ranging from no enhancement to 100% enhancement.

3D quantitative image analysis was performed using a software prototype (Medisys Research Lab, Philips Healthcare, Suresnes, France) (18). The software employed a semiautomatic 3D tumor segmentation using non-Euclidean radial basis functions on the contrast-enhanced MR imaging (Fig 1a, b). The TLV was directly calculated based on this 3D segmentation (Fig 1c). The volumetric accuracy and reader-independent reproducibility of the segmentation software used has been previously reported (19,20). Subsequently, the resulting 3D segmentation mask was used for the quantitative evaluation of fibroid response to embolization on contrast-enhanced arterial-phase MR imaging. The calculation was based on image subtraction and used the following algorithm: (*i*) The MR imaging scan performed before contrast enhancement was subtracted from the arterial-phase scan to remove background enhancement to differentiate automatically residual enhancement from hemorrhagic infarction. (*ii*) The 3D segmentation mask was transferred to the subtraction image. (*iii*) A region of interest (ROI; 1 cm^3) was placed on hypoenhancing soft tissue (the left psoas muscle was selected as a reference) to calculate a normalized threshold for tissue enhancement (Fig 1d). (*iv*) Enhancing fibroid tissue was defined as voxels within the 3D mask where the enhancement exceeded the average plus twice the SD value of the ROI. (*v*) To estimate fibroid infarction, nonenhancing and hypoenhancing areas were assumed to be largely necrotic, and the ELV was expressed in cubic centimeters and a percentage of the previously calculated TLV. (*vi*) A color map overlay normalized to the maximum intensity in the contrast-enhanced MR imaging scan per patient was used to demonstrate the distribution and intensity of the enhancement (Fig 1d). This algorithm was used for both baseline (Fig 1a–d) and follow-up contrast-enhanced MR imaging (Fig 1e, f). Appendix A (available online at www.jvir.org) contains additional information for the segmentation technique, workflow and time efficiency, calculations of the enhancing fibroid volume, ROI statistics, and color map coding.

Statistical Analysis

All statistical calculations were performed using the commercially available statistical software GraphPad Prism (Version 6; GraphPad Software, San Diego, California). Descriptive statistics were used to summarize the data. Count and frequency were used for categorical variables. Mean and range were used for continuous variables. A linear regression model was used to analyze the correlation of results from 3D quantitative measurements and subjective radiologic readings. Pearson correlation coefficient (R^2) was calculated. In addition, residual plots were used to assess drift, variance, and deviation. The

residual standard error was calculated to measure the discrepancy between the software-assisted and manual measurements. The *t* test and the Wilcoxon test for paired samples were used to compare the parameters between patient groups and in individual patients before and after treatment. A P value < .05 was considered statistically significant.

RESULTS

Baseline Patient Characteristics

The Table summarizes baseline characteristics of the selected patients. All 25 patients underwent technically successful bilateral UAE. No complications during or after the procedure were recorded. No patient underwent reintervention, and none showed worsened clinical symptoms after the procedure. Analysis of clinical outcome revealed that menorrhagia and bulk-related symptoms improved in 15 patients (60%) at first follow-up compared with baseline assessment. Disease-related symptoms improved or resolved in 19 patients (76%) on second follow-up examination. This group of patients (n = 19) was classified as responders to UAE. However, six patients (24%) showed no improvement of symptoms of menorrhagia, bulk-related symptoms, or both by the second follow-up examination. These patients were classified as nonresponders.

Within the group of patients who were excluded because of lack of follow-up MR imaging, 73% (38 of 52) of patients presented for clinical follow-up evaluation within 24 months after treatment. Within this group, 92% (35 of 38) qualified as clinical responders and did not require further treatment. Of patients without MR imaging after treatment, 27% (14 of 52) were lost to follow-up.

Quantification of Lesion Volume

Measurements of the TLV calculated with the software-assisted, semiautomated 3D technique were compared with manually recorded values. As a result, software-assisted measurements showed a strong correlation with manually measured TLV for baseline imaging (R^2 = 0.9638) (Fig 2a) and follow-up MR imaging (R^2 = 0.9301) (Fig 2b). The mean TLV on baseline MR imaging according to software-assisted measurements was 189 cm^3 (median volume, 126 cm^3; range, 5–552 cm^3) (Fig 2c). The software-based analysis of volumetric changes after UAE showed a statistically significant reduction of TLV in all patients (P < .01) (Fig 2c). After the procedure, mean TLV on follow-up MR imaging was 116 cm^3 (median, 79 cm^3; range, 0.6–341 cm^3) (Fig 2c). When stratified according to clinical symptoms, mean TLV after the procedure in the group of responders (mean, 67 cm^3; median, 59 cm^3; range, 0.6–209 cm^3) appeared to be significantly smaller compared with nonresponders (mean, 204 cm^3; median, 194 cm^3, range, 66–341 cm^3) (Fig 2d). The software-assisted, segmentation-based 3D assessment of TLV has demonstrated strong agreement with manual measurements, providing a foundation for the quantification of lesion enhancement within the volume of interest.

Quantification of Lesion Enhancement

The feasibility of the software-assisted technique to quantify fibroid infarction as a surrogate or predictive marker for UAE efficacy was tested using follow-up MR imaging. For this

purpose, software-assisted measurements of fibroid enhancement were correlated with the values recorded during the visual assessment of the enhancing fibroid portions. Results from both approaches showed some correlation (R^2 = 0.724) (Fig 3a). However, residual analysis revealed major disagreement between both techniques with a high variance of up to 38% and a residual standard error of 15.8 (Fig 3b). The software-assisted technique provided two metrics to quantify the enhancing portion of the fibroid: (*a*) ELV in cm^3 and (*b*) percentage of ELV relative to the TLV. Both output systems were used to analyze the changes of fibroid enhancement before and after UAE (Fig 4a, b). According to the relative percentage values (ELV/TLV), all patients showed fibroid infarction after UAE with a mean of 41% enhancement on follow-up MR imaging (median, 39%; range, 4%–97%) (Fig 3b). When quantified using the absolute metric, all assessed lesions showed significant reduction of ELV to a mean of 43 cm^3 (median, 15 cm^3; range 0.3–296 cm^3) (Fig 4a). A stratification of fibroid enhancement on follow-up MR imaging according to clinical results was performed. When stratified according to percentage (ELV/TLV), no significant difference between responders and nonresponders was apparent (*P* .05) (Fig 4d). However, quantification using the absolute ELV (in cm^3) resulted in a statistically significant difference between the two clinical groups (*P* = .025) (Fig 4c). Responders showed a mean ELV of 4.1 cm^3 (median, 4.7 cm^3; range, 0.3–19.8 cm^3), whereas nonresponders appeared to have a higher mean ELV of 75 cm^3 (median, 41 cm^3; range, 11.91–296 cm^3) after UAE. None of the patients with < 10 cm^3 of ELV (n = 11) after UAE was a nonresponder, whereas 43% (n = 6) of patients with > 10 cm^3 of ELV (n = 14) were nonresponders. The quantification of the enhancing lesion volume using relative software-based metrics showed some disagreement with conventional, visual measurements and no correlation with clinical outcome, whereas the absolute metrics demonstrated significant differences between symptomatic responders and nonresponders.

DISCUSSION

The main finding of this pilot study is that 3D quantitative evaluation of uterine fibroid response to embolization using contrast-enhanced MR imaging is clinically feasible and diagnostically accurate. Although demonstrating a good intermethod correlation for the quantification of the total lesion volumes, the enhancement-based component of the semiautomated 3D technique showed significant disagreement with the subjective assessment method and concurrently provided a better correlation with clinical outcome after UAE.

Clinical outcome after UAE continues to be the ultimate endpoint in most prospective and retrospective studies. However, several studies established the role of fibroid enhancement after UAE on contrast-enhanced MR imaging, a surrogate for the extent of infarction, as a predictor of clinical outcome (9,21). Specifically, incomplete fibroid infarction has been shown to result in symptom recurrence and the need for repeat embolization (12,13). Quantification of fibroid viability has largely relied on manual measurements or subjective, visual assessment of fibroid enhancement. The visual quantification of enhancing tissue usually results in relative metrics such as the percentage of the TLV (13,22). This approach has two major limitations: First, the reproducibility and reliability of subjective measurements are strongly dependent on the individual observer, potentially introducing a

high interobserver variability (22); second, non-3D quantitative techniques are susceptible to numerical output bias when calculating enhancement as percentage of the entire lesion, neglecting the impact of lesion shrinkage over time and the absolute burden of the remaining viable fibroid tissue. Both limitations may have contributed to rising doubts as to whether conventionally analyzed contrast-enhanced MR imaging performed after UAE is capable of predicting or even correlating with clinical outcome (15,23). The 3D quantitative technique described here addresses both limitations. First, semiautomated lesion segmentation is known to be a highly reproducible and reliable technique, tested in uterine fibroids and other solid tumors (19,22). Second, a threshold-based, voxel-by-voxel analysis of ELV is capable of providing absolute numeric values in cubic centimeters. The benefit of this approach lies in its ability to reflect the absolute burden of biologically viable tissue with regrowth potential within incompletely infarcted lesions. Most importantly, it was observed that although manual measurements of the TLV appeared to be closely associated with results from the semiautomatic technique, the assessment of fibroid enhancement showed a great extent of disagreement between the software-assisted and the visual assessment technique. This disagreement can be explained by the asymmetry of fibroid infarction, which in many cases shows central necrosis and rim and segmental enhancement with scattered foci of remaining viable fibroid tissue, making visual assessment susceptible to imprecision and implying the benefits of 3D quantitative analysis.

From a pathologic standpoint, uterine fibroid response to UAE occurs gradually. Although fibroid necrosis is known to occur within 72 hours after embolization, lesion shrinkage may follow over a period of several weeks (14,24,25). These changes can be observed on contrast-enhanced MR imaging immediately after the procedure and on late follow-up scans (4–12 mo after treatment) (9). Reporting enhancement as a percentage of the entire lesion may be accurate only for the former and proved clinically irrelevant for lesions that have changed in size. Also, this approach might be misleading when comparing lesion enhancement on contrast-enhanced MR imaging performed early versus late after the procedure (this is further illustrated in Fig E1a, b, available online at www.jvir.org). This assumption is supported by the results of this study, which demonstrate the failure of the relative assessment (ELV/TLV in %) to correlate with clinical outcome, while confirming the benefit of absolute metrics (ELV in cm^3). The use of absolute volumes, measured by a segmentation-based technique, may be considered a diagnostically more accurate and clinically more relevant approach in assessing fibroid enhancement.

This pilot study has several limitations. First, the retrospective design of the study has prevented an evaluation of patients with follow-up MR imaging acquired according to a well-scheduled protocol. However, the included patients showed a reasonably tight distribution of follow-up MR imaging scans with most (84%) of the included patients undergoing scanning 6 months after treatment. Second, the retrospective character of the study and the relatively small population of consecutively treated patients are drawbacks regarding a more elaborate stratification of clinical symptoms. This limitation was countered with a stratification of clinical outcome in two major subgroups of patients (responders and nonresponders). The overall nonresponder rate of 24% in this study is slightly above the reported average of 10%–15% (24). This larger nonresponder rate can be explained by the large dropout rate of patients who did not present for imaging after UAE, most of whom

qualified as responders in clinical follow-up examinations. A third limitation is the lack of radiologic-pathologic correlation for our imaging results. This limitation is of great importance in light of the significant disagreement between the manual and the 3D quantitative assessment of lesion enhancement and viability because our study could not confirm the suggested advantage of the semiautomated technique in the assessment of lesion necrosis while indicating the clinical benefits of this technique. However, collecting pathologically assessable fibroid tissue is nearly impossible precisely because of the character of UAE as an alternative to surgical techniques. Additionally, the 3D quantitative instruments used in this study were subject to validation with regard to their volumetric accuracy and were deemed sufficiently reliable for the scope of this analysis. Finally, a fourth limitation of the presented approach is the selection of the dominant lesions as surrogates for the overall response. As opposed to other intraarterial embolization procedures, UAE is not selective and does not follow the premise of a lesion-by-lesion treatment and instead aims at achieving a global response, which may suggest the use of a representative lesion for imaging purposes. No published evidence exists that would demonstrate technical benefits of assessing multiple lesions over the assessment of a single, representative lesion in uterine fibroids. In addition, current segmentation techniques do not yet allow a workflow-efficient 3D analysis of multiple uterine fibroids. The minimum number of lesions needed for analysis remains an open question, and future studies may evaluate potential benefits of a multiple-lesion analysis.

In conclusion, this feasibility study provides initial evidence for the advantage of a semiautomatic, 3D quantitative technique to assess fibroid response after UAE. Our results underline the limitations of the most commonly used techniques of reporting lesion enhancement. The presented results are preliminary and require further validation using a larger cohort of prospectively enrolled patients with sequential MR imaging acquisition. In addition, clinical outcome will likely continue to be the most significant endpoint of therapy of uterine fibroids. However, once fully validated, the absolute metrics and a higher diagnostic accuracy of the software-assisted technique may help predict long-term clinical outcome based on contrast-enhanced MR imaging performed after the procedure.

Supplementary Material

Refer to Web version on PubMed Central for supplementary material.

Acknowledgments

This study was funded by National Institutes of Health Grant (NIH/NCI R01 CA160771, P30 CA0069730) as well as Philips Research North America, Briarcliff Manor, New York, French Society of Radiology, and Rolf W. Günther Foundation for Radiological Science. The authors acknowledge the contributions of Stacey A. Scheib, MD, and Mark Zakaria, MD.

ABBREVIATIONS

ELV	enhancing lesion volume
ROI	region of interest

3D	three-dimensional
TLV	total lesion volume
UAE	uterine artery embolization

References

1. American College of Obstetricians and Gynecologists. ACOG practice bulletin. Alternatives to hysterectomy in the management of leiomyomas. Obstet Gynecol. 2008; 112:387–400. [PubMed: 18669742]
2. Ravina JH, Herbreteau D, Ciraru-Vigneron N, et al. Arterial embolisation to treat uterine myomata. Lancet. 1995; 346:671–672. [PubMed: 7544859]
3. Goodwin SC, Spies JB, Worthington-Kirsch R, et al. Uterine artery embolization for treatment of leiomyomata: long-term outcomes from the FIBROID Registry. Obstet Gynecol. 2008; 111:22–33. [PubMed: 18165389]
4. Hehenkamp WJ, Volkers NA, Birnie E, Reekers JA, Ankum WM. Symptomatic uterine fibroids: treatment with uterine artery embolization or hysterectomy—results from the randomized clinical Embolisation versus Hysterectomy (EMMY) trial. Radiology. 2008; 246:823–832. [PubMed: 18187401]
5. Scheurig-Muenkler C, Koesters C, Powerski MJ, Grieser C, Froeling V, Kroencke TJ. Clinical long-term outcome after uterine artery embolization: sustained symptom control and improvement of quality of life. J Vasc Interv Radiol. 2013; 24:765–771. [PubMed: 23582992]
6. Hovsepian DM, Siskin GP, Bonn J, et al. Quality improvement guidelines for uterine artery embolization for symptomatic leiomyomata. J Vasc Interv Radiol. 2009; 20:S193–S199. [PubMed: 19559999]
7. deSouza NM, Williams AD. Uterine arterial embolization for leiomyomas: perfusion and volume changes at MR imaging and relation to clinical outcome. Radiology. 2002; 222:367–374. [PubMed: 11818601]
8. Spies JB, Roth AR, Jha RC, et al. Leiomyomata treated with uterine artery embolization: factors associated with successful symptom and imaging outcome. Radiology. 2002; 222:45–52. [PubMed: 11756703]
9. Kroencke TJ, Scheurig C, Poellinger A, Gronewold M, Hamm B. Uterine artery embolization for leiomyomas: percentage of infarction predicts clinical outcome. Radiology. 2010; 255:834–841. [PubMed: 20392986]
10. Chrisman HB, West D, Corpuz B, et al. Primary failure of uterine artery embolization: use of magnetic resonance imaging to select patients for repeated embolization. J Vasc Interv Radiol. 2005; 16:1143–1147. [PubMed: 16105928]
11. Katsumori T, Kasahara T, Kin Y, Nozaki T. Infarction of uterine fibroids after embolization: relationship between postprocedural enhanced MRI findings and long-term clinical outcomes. Cardiovasc Intervent Radiol. 2008; 31:66–72. [PubMed: 17943351]
12. Yousefi S, Czeyda-Pommersheim F, White AM, Banovac F, Hahn WY, Spies JB. Repeat uterine artery embolization: indications and technical findings. J Vasc Interv Radiol. 2006; 17:1923–1929. [PubMed: 17185687]
13. Pelage JP, Guaou NG, Jha RC, Ascher SM, Spies JB. Uterine fibroid tumors: long-term MR imaging outcome after embolization. Radiology. 2004; 230:803–809. [PubMed: 14990844]
14. Deshmukh SP, Gonsalves CF, Guglielmo FF, Mitchell DG. Role of MR imaging of uterine leiomyomas before and after embolization. Radiographics. 2012; 32:E251–E281. [PubMed: 23065174]
15. Koesters C, Powerski MJ, Froeling V, Kroencke TJ, Scheurig-Muenkler C. Uterine artery embolization in single symptomatic leiomyoma: do anatomical imaging criteria predict clinical presentation and long-term outcome? Acta Radiol. 2014; 55:441–449. [PubMed: 23943627]

16. Bossuyt PM, Reitsma JB, Bruns DE, et al. Towards complete and accurate reporting of studies of diagnostic accuracy: the STARD initiative. Radiology. 2003; 226:24–28. [PubMed: 12511664]
17. Coyne KS, Margolis MK, Bradley LD, Guido R, Maxwell GL, Spies JB. Further validation of the uterine fibroid symptom and quality-of-life questionnaire. Value Health. 2012; 15:135–142. [PubMed: 22264981]
18. Lin M, Pellerin O, Bhagat N, et al. Quantitative and volumetric European Association for the Study of the Liver and Response Evaluation Criteria in Solid Tumors measurements: feasibility of a semiautomated software method to assess tumor response after transcatheter arterial chemoembolization. J Vasc Interv Radiol. 2012; 23:1629–1637. [PubMed: 23177109]
19. Tacher V, Lin M, Chao M, et al. Semiautomatic volumetric tumor segmentation for hepatocellular carcinoma: comparison between C-arm cone beam computed tomography and MRI. Acad Radiol. 2013; 20:446–452. [PubMed: 23498985]
20. Pellerin O, Lin M, Bhagat N, Ardon R, Mory B, Geschwind JF. Comparison of semi-automatic volumetric VX2 hepatic tumor segmentation from cone beam CT and multi-detector CT with histology in rabbit models. Acad Radiol. 2013; 20:115–121. [PubMed: 22947274]
21. Scheurig-Muenkler C, Koesters C, Grieser C, Hamm B, Kroencke TJ. Treatment failure after uterine artery embolization: prospective cohort study with multifactorial analysis of possible predictors of long-term outcome. Eur J Radiol. 2012; 81:e727–e731. [PubMed: 22381440]
22. Heye T, Merkle EM, Reiner CS, et al. Reproducibility of dynamic contrast-enhanced MR imaging. Part II: comparison of intra- and interobserver variability with manual region of interest placement versus semi-automatic lesion segmentation and histogram analysis. Radiology. 2013; 266:812–821. [PubMed: 23220891]
23. Hecht EM, Do RK, Kang SK, Bennett GL, Babb JS, Clark TW. Diffusion-weighted imaging for prediction of volumetric response of leiomyomas following uterine artery embolization: a preliminary study. J Magn Reson Imaging. 2011; 33:641–646. [PubMed: 21563247]
24. Bulman JC, Ascher SM, Spies JB. Current concepts in uterine fibroid embolization. Radiographics. 2012; 32:1735–1750. [PubMed: 23065167]
25. Kirby JM, Burrows D, Haider E, Maizlin Z, Midia M. Utility of MRI before and after uterine fibroid embolization: why to do it and what to look for. Cardiovasc Intervent Radiol. 2011; 34:705–716. [PubMed: 21085962]

APPENDIX A

Lesion Segmentation

To optimize the accuracy of fibroid segmentation, a systematic approach was used. A semiautomatic 3D segmentation of the lesions was performed using a contrast-enhanced MR imaging sequence obtained before and at follow-up after UAE. The lesion segmentation was performed using an in-house software program (Medisys Research Lab, Philips Healthcare, Suresnes, France). This software uses non-Euclidean geometry and theory of radial basis functions, which allows the segmentation of 3D objects with straight edges and corners (19). The algorithm creates image-based masks located in a 3D region the center and size of which are defined by the user, yielding the nomenclature “semiautomatic.” After identifying an initial control point, the user can interactively expand or contract the 3D mask. Adjustments of the overall 3D volume of the mask can be interactively performed by placing additional control points. The shape and the spatial localization of the final 3D segmented mask (Fig 1c, d) are registered to the coordinates within the MR imaging dataset and—on image registration—may be applied to other MR imaging scans of the same patient. With the 3D nature of the segmentation, the tumor volume can be directly calculated. The workflow efficiency of the segmentation system has been tested by recording the time needed to segment a lesion. For a total of 25 lesions and 50

segmentations, the average time/segmentation was 31 seconds (range, 7–120 s). Empirically, segmentation of larger lesions or lesions with ill-defined borders was more time-consuming.

Software-Assisted Assessment of Lesion Enhancement

To quantify fibroid enhancement using the software-assisted technique, the following steps were performed:

1. The MR imaging scan performed before contrast enhancement was subtracted from the contrast-enhanced MR imaging scan to remove background enhancement. This step is important to achieve an accurate assessment of lesions with potentially hemorrhagic necrosis and helps mitigate false-positive enhancement from contrast enhancement.
2. The 3D segmentation mask was transposed onto the subtracted image set.
3. A 3D ROI of 1 cm^3 was placed into nonenhancing soft tissue (left psoas muscle) of the subtracted image set to calculate the relative enhancement values within the lesion volume as a reference for normalization (Fig 1d). The placement was carefully performed to avoid any adjacent main branch blood vessels or motion artifacts. Additional information on the selection of ROIs is provided in the following section (“Definition of ROI and Color Coding”).
4. A threshold based on image enhancement defined viable lesion tissue as voxels within the 3D mask where the enhancement exceeded the average + 2 SD value of the ROI. Additional information on the calculation of the ROI-based threshold is provided in the following section.
5. To estimate lesion enhancement, enhancing regions of the tumor (voxels with enhancement greater than the ROI threshold) were assumed to be largely viable and expressed in cubic centimeters.
6. A normalized color map overlay on the MR imaging scan was used to demonstrate regional lesion enhancement heterogeneity (Fig 1d, f, with red representing maximum enhancement or viable fibroid and blue representing no enhancement, below the threshold or necrotic tissue) (18). Additional information on color coding is provided in the following section.

Definition of ROI and Color Coding

As opposed to fully automated segmentation techniques, a semiautomated approach allows the combination of software-based image processing with manual adjustments by a radiologic reader. The goal of the ROI selection in this study was to achieve an intuitive approach, resembling the gold standard of a radiologic reading. Practically, a radiologic reader compares enhancement properties of the lesions with the nonenhancing soft tissue. Several ROI localizations (including healthy uterine tissue, several muscles, and fat) were considered; however, they appeared to be counterintuitive and failed to provide consistent results for all patients, whereas the psoas muscle appeared to be easily reproducible and provided a consistently nonenhancing soft tissue reference. To avoid corrupted ROIs within

focally inhomogeneous muscle tissue, signal intensity statistics were calculated for every 3D (1 cm × 1 cm × 1 cm = 1 cm^3) ROI with the goal of achieving a maximum of signal homogeneity. This calculation was performed as follows:

1. A 1 cm^3 ROI was placed in a localization as described earlier.
2. The software provided the minimum and maximum voxel brightness values within the cubic ROI. The numeric output was in patient-specific arbitrary units for each ROI. The software calculated the mean brightness value (MBV), SD, and coefficient of variation. Empirically, a coefficient of variation of < 30% was seen as acceptable, whereas a CV > 30% was rejected leading to ROI repositioning.
3. The MBV ± 2 SD was selected as a cutoff (threshold) with all values above seen as real contrast enhancement. Areas greater than the threshold (enhancing) were categorized as viable.
4. Based on the selected ROI and the MBV, a patient-specific (normalized) 3D color map was overlaid onto the tumor tissue enclosed by the segmentation mask. The color blue was identified as areas with equal or lower signal intensity as the MBV ± 2 SD, whereas all signal exceeding this value was coded as an equally distributed histogram of tissue enhancement.

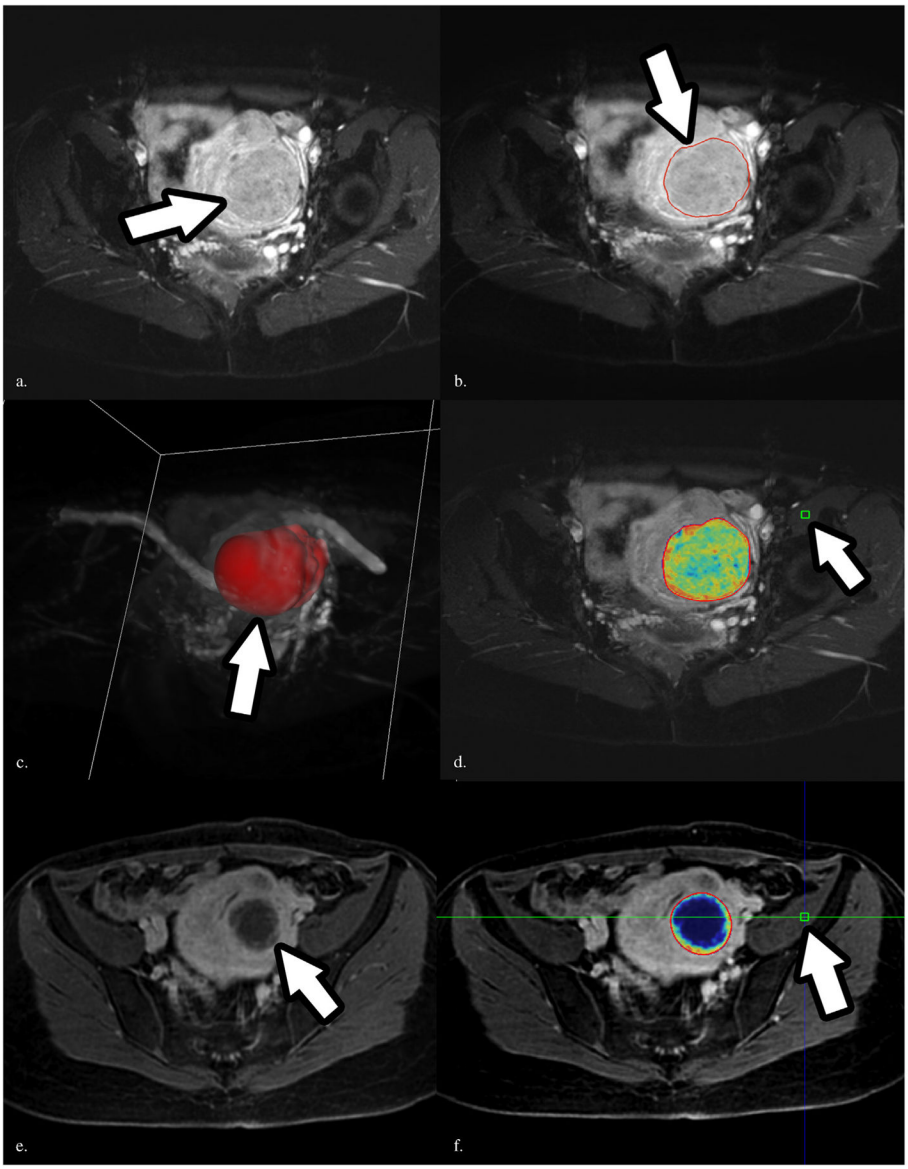

Figure 1.

Software-assisted 3D quantification technique. **(a)** Representative contrast-enhanced MR imaging scan performed before the procedure. Arrow points to dominant fibroid lesion. **(b)** Semiautomated tumor segmentation, which includes the entire lesion on the scan performed before the procedure. Arrow indicates the rim of the segmented lesion. **(c)** Volume rendering for the segmented lesion in a maximum intensity projection on the scan performed before the procedure. Arrow indicates the lesion (in red). **(d)** Color map of the same lesion before UAE; the color coding varies from red representing maximum enhancement to blue representing no enhancement. Arrow indicates the ROI within the left psoas muscle, which was used as a reference. **(e, f)** Contrast-enhanced follow-up MR imaging scans from the same patient after UAE, with and without the color map overlay. Arrow in **(e)** indicates the centrally necrotic uterine fibroid. Arrow in **(f)** indicates the ROI, consistently placed within the left psoas muscle.

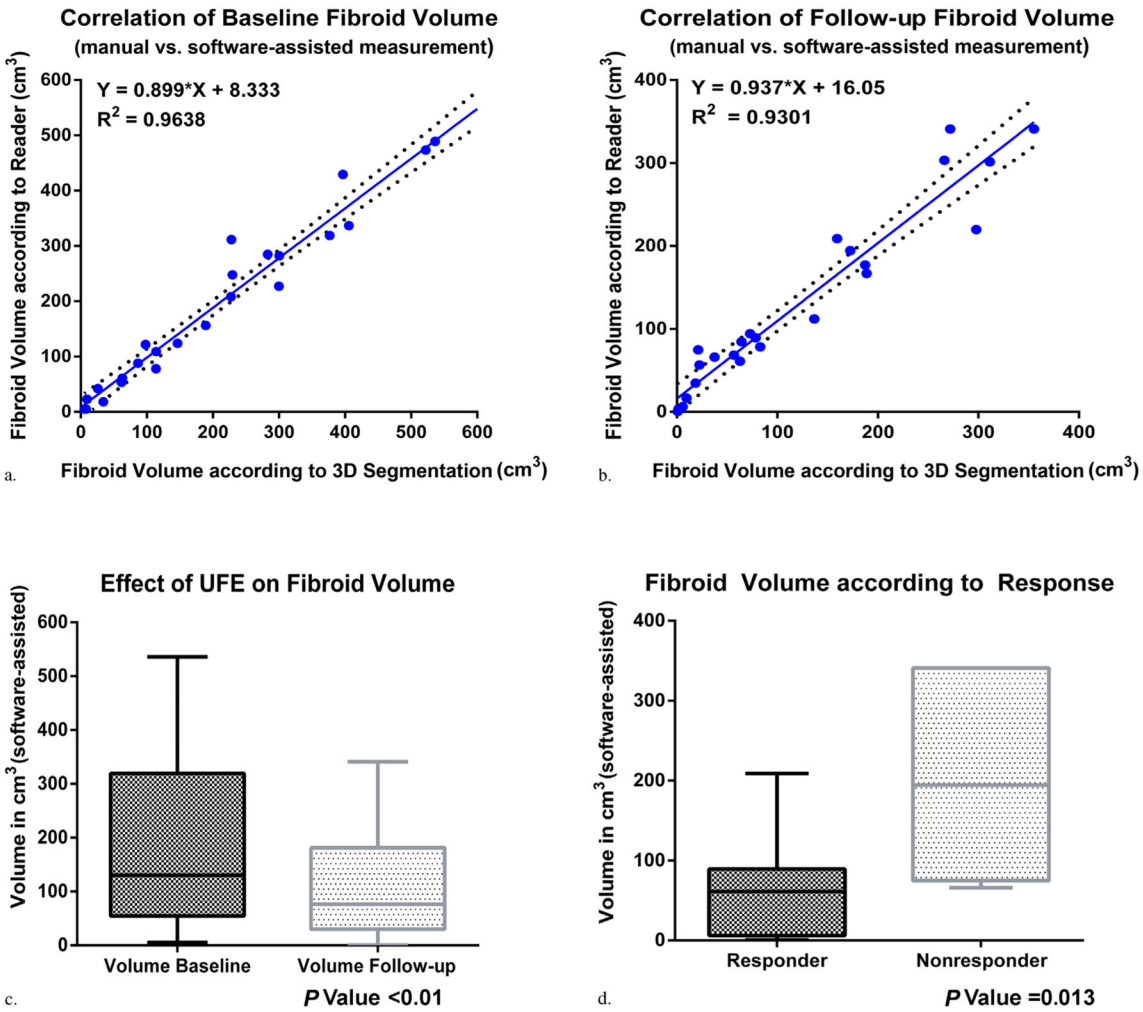

Figure 2.

Quantification of fibroid volume. **(a, b)** Correlation between the semiautomatic assessment and manual measurements for baseline and follow-up MR imaging scans. **(c)** Overall effects of uterine fibroid embolization (UFE) on lesion volume, assessed using the software-assisted technique. **(d)** Stratification of volumetry values between responders and nonresponders on follow-up imaging. (Available in color online at www.jvir.org.)

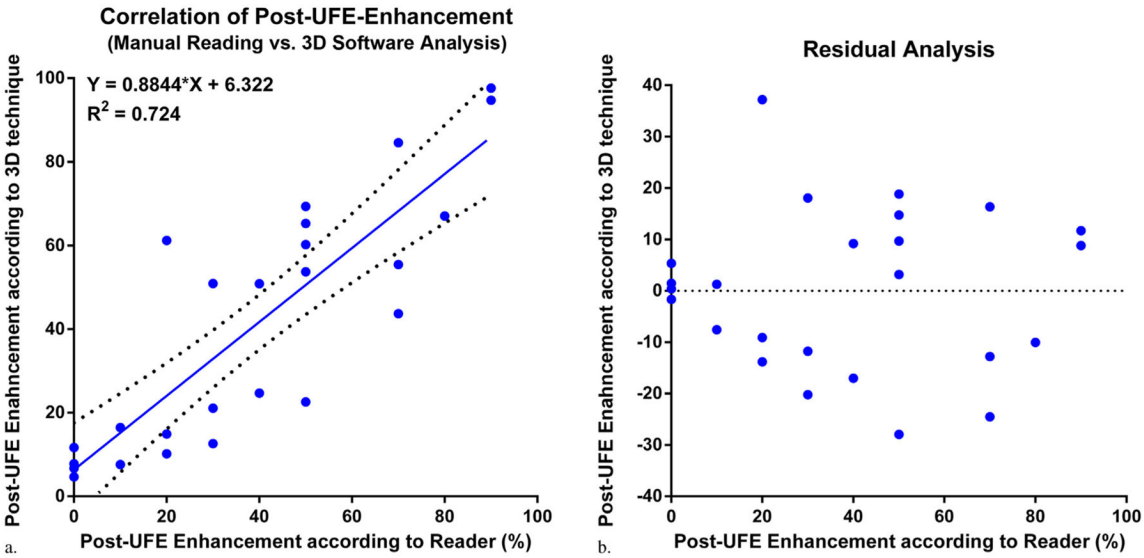

Figure 3.

Visual versus semiautomated quantification of fibroid enhancement. **(a)** The graph illustrates the correlation between visual and software-assisted measurements of fibroid enhancement on follow-up MR imaging. **(b)** The graph demonstrates the residuals resulting from the correlation under **(a)**. UFE = uterine fibroid embolization. (Available in color online at www.jvir.org.)

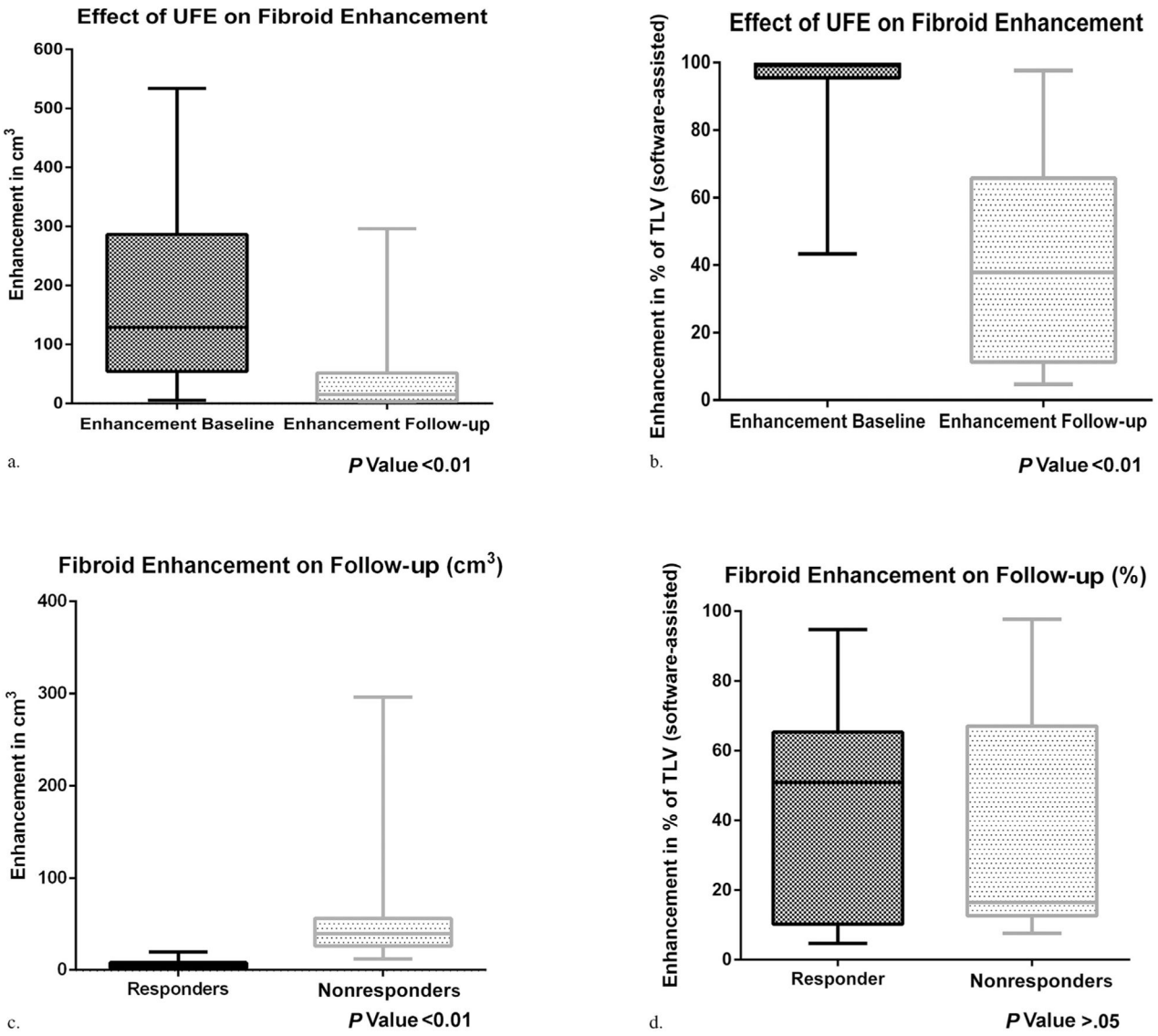

Figure 4.

Software-assisted quantification of fibroid enhancement. **(a, b)** Comparison of fibroid enhancement measured on contrast-enhanced baseline and follow-up MR imaging. **(c, d)** Stratification of the same values on follow-up imaging according to clinical patient response. The quantification using absolute units (cm^3) shows significant differences between the groups. When assessed according to percentage of TLV, no significant difference between the groups is apparent.

Table

Patient Characteristics

Parameter	N (Range/%)
Age (y)	46* (40–54)
Race	
African-American	17 (68)
White	7 (28)
Asian	1 (4)
Symptoms at presentation	
Menorrhagia	25 (100)
Bulk-related	23 (92)
No. uterine fibroids	
1	2 (8)
2–5	14 (56)
> 5	9 (36)
Dominant fibroid location	
Subserosal	6 (24)
Intramural	17 (68)
Submucosal	2 (8)
Baseline volume (cm^3)	189* (5–522)

*Mean.